



Non-local continuum modeling of carbon nanotubes: Physical interpretation of non-local kernels using atomistic simulations

Veera Sundararaghavan*, Anthony Waas*

Department of Aerospace Engineering, University of Michigan, Ann Arbor MI 48109, United States

ARTICLE INFO

Article history:

Received 1 September 2010

Received in revised form

5 March 2011

Accepted 15 March 2011

Available online 29 March 2011

Keywords:

Carbon nanotubes

Phonon dispersion

Wave propagation

Non-local elasticity

Shell theory

ABSTRACT

The longitudinal, transverse and torsional wave dispersion curves in single walled carbon nanotubes (SWCNT) are used to estimate the non-local kernel for use in continuum elasticity models of nanotubes. The dispersion data for an armchair (10,10) SWCNT was obtained using lattice dynamics of SWNTs while accounting for the helical symmetry of the tubes. In our approach, the Fourier transformed kernel of non-local linear elastic theory is directly estimated by matching the atomistic data to the dispersion curves predicted from non-local 1D rod theory and axisymmetric shell theory. We found that gradient models incur significant errors in both the phase and group velocity when compared to the atomistic model. Complementing these studies, we have also performed detailed tests on the effect of length of the nanotube on the axial and shear moduli to gain a better physical insight on the nature of the true non-local kernel. We note that unlike the kernel from gradient theory, the numerically fitted kernel becomes negative at larger distances from the reference point. We postulate and confirm that the fitted kernel changes sign close to the inflection point of the interatomic potential. The numerically computed kernels obtained from this study will aid in the development of improved and efficient continuum models for predicting the mechanical response of CNTs.

© 2011 Elsevier Ltd. All rights reserved.

1. Introduction

Non-local continuum field theories are concerned with the physics of material bodies whose behavior at a material point is influenced by the state of all points that constitute the body. For homogeneous and isotropic elastic solids with zero body forces, the non-local field theory is expressed by the following governing equations:

$$s_{ij,i} = \rho \ddot{u}_j \quad (1)$$

$$s_{ij}(\mathbf{x}) = \int_V \alpha(|\mathbf{x}' - \mathbf{x}|) \sigma_{ij}(\mathbf{x}') dV(\mathbf{x}') \quad (2)$$

$$\sigma_{ij}(\mathbf{x}') = C_{ijkl} \varepsilon_{kl}(\mathbf{x}') \quad (3)$$

$$\varepsilon_{ij}(\mathbf{x}') = \frac{1}{2} \left(\frac{\partial u_i(\mathbf{x}')}{\partial x_j'} + \frac{\partial u_j(\mathbf{x}')}{\partial x_i'} \right) \quad (4)$$

where s_{ij} and σ_{ij} are stress tensors, and ε_{ij} is the strain tensor. C_{ijkl} is the elastic modulus tensor in classical elasticity theory and u_i is the displacement vector, and the integration in Eq. (2) is carried over the volume, V , of the body. Non-local theory

* Corresponding authors.

E-mail addresses: veeras@umich.edu (V. Sundararaghavan), dcw@umich.edu (A.M. Waas).

proposed by Eringen (1983), assumes that stress (\mathbf{s}) at a material point depends on the classical local stresses, σ_{ij} , induced by deformation within a *finite volume*, V , surrounding the material point, by means of a non-local kernel α (a function of Euclidean distance $|\mathbf{x}-\mathbf{x}'|$) that weights the classical stresses around point \mathbf{x} . Note that the volume V entering Eq. (2) is smaller than the total volume of the body. The non-local weighting kernel α satisfies three important properties: firstly it is maximum at the point of interest and decays around it; secondly, the kernel is normalized with respect to the volume V ($\int_V \alpha dV = 1$), so that α reverts to a delta function as the zone of influence vanishes which leads to the classical (local) elasticity formulation. Non-local theories nominally take into account the multi-atom interactions that determine the stress state at a point. Thus, non-local elasticity can overcome several issues associated with local elasticity, for example, local elasticity does not predict the effect of material size on elastic moduli (the size effect, eg. Aifantis,).

The application of non-local elasticity to model nanoscale materials has emerged as an important topic recently, due to the limit on computational resources that inhibit large scale computations using fine scale models such as molecular dynamics. Much attention has been focussed on correctly capturing the physical properties of Carbon nanotubes in developing constitutive models. Nanotubes are expected to be as stiff as graphite along the graphene layers or even reach the stiffness of diamond. This unique mechanical property of the nanotubes combined with their lightness predetermines their usage in composite materials and has motivated computational studies of their constitutive behavior. Application of nonlocal theory to study the bending, vibration and buckling behavior of Carbon nanotubes (CNTs) (Peddieson et al., 2003; Kumar et al., 2008; Sudak, 2003; Sun and Zhang, 2003; Zhang et al., 2005) has been advanced recently using stress and strain gradient theories, which are special forms of non-local theory derived from a special class of kernels. For example, for 2D lattices, $\alpha = (2\pi c^2)^{-1} K_0(\sqrt{\mathbf{x} \cdot \mathbf{x}}/c)$, where K_0 is the modified Bessel function, and it satisfies the differential equation: $(1-c^2 \nabla^2)\alpha = \delta(|\mathbf{x}|)$. The application of this equation to the integral formulation described previously leads to the constitutive relationship in gradient elasticity $(1-c^2 \nabla^2)\mathbf{s} = \boldsymbol{\sigma}$. The parameter c was explained by Eringen as a product of a material specific parameter (e_0) and an internal characteristic length (a). The gradient formulation has been shown to reasonably reproduce the phonon dispersion curve for a Born–Karman model of lattice dynamics (harmonic spring model). However, nanotubes have complex lattice dynamics and the use of simplified gradient theories to model phenomena such as size effect in nanotube needs further detailed study.

Both theoretical analyses and numerical simulations have revealed that wave dispersion relations in the longitudinal and circumferential directions have non-local effects. Wang et al. have studied several vibration problems of nanotubes based on Flugge elastic shell theory (Wang et al., 2005; Wang and Varadan, 2007; Hu et al., 2008). In a recent study, Wang et al. (2005), it was found that the best fit kernel parameter (e_0) changes depending on which atomistically computed vibration modes are fitted to the shell theory (for instance, for transverse vibrations, ($e_0 = 0.2$) and for torsional vibrations, ($e_0 = 0.4$)). These results present an atomistically validated form of kernel for CNTs; nevertheless the kernel is approximated within the gradient theory and the exact form is not calculated. For a special case of interatomic potentials depending only on pair interactions (or through embedded functions that are function of radial distance only), a direct reconstruction technique for the kernel based on potential description was proposed by Picu (2002). However, such approaches cannot be used for CNTs since carbon atom interactions in CNT are typically multibody potentials that depend on atom coordination (Brenner potential) or three or four body interactions (Force field potentials).

In this paper, we follow the approach suggested originally by Eringen (1983), to directly compute the *fourier transformed* kernel through fitting the predictions of a model kernel with the phonon dispersion curve of the CNT lattice. The Fourier transformed non-local kernel is reproduced for two specific models of nanotube prevalent in literature, the 1D beam model and the axisymmetric shell model based on Flugge theory. The new data from this work can be further used to refine a variety of non-local models for use in nanotube analysis. To this end, we have provided a detailed atomistic study of size effect of moduli with respect to nanotube length (different from size effect with respect to nanotube diameter studied in Wang et al., 2005). We find that the elastic moduli is lower in shorter nanotubes due to increased influence of uncoordinated edge atoms. In order to better understand the physical nature of the non-local kernel, atomistic data was used to compute a new Gaussian-type kernel. The computed kernel is seen to become negative at larger distances from the reference point, unlike the stress gradient theory. We postulate that the kernel changes sign close to the inflection point of the interatomic potential. This postulate is confirmed through an atomistic study of layer-by-layer interaction of atoms in a carbon nanotube. The study thus provides new insight into the nature of the non-local kernel of a CNT.

The paper is arranged as follows. In Section 2, the essential features of a model of the lattice dynamics of SWNTs based on the explicit accounting for the helical symmetry of the tubes are summarized. The phonon dispersion curves for the nanotube computed from this approach are used to obtain the expression for $\alpha(k)$ (the Fourier transform of the non-local kernel) through comparison with the 1D beam theory and non-local axisymmetric shell theory in Sections 3 and 4, respectively. Finally, in Section 5, we provide physical interpretation of the obtained kernel parameters by comparing the theory with elastic and shear moduli variation with the length of the nanotube predicted from atomistic calculations. We also predict the possibility of negative kernel weights through atomistic simulations.

2. Atomistic modeling of dispersion curves of nanotubes

The ideal nanotube structure can be obtained from a graphene sheet by rolling it up along a straight line connecting two lattice points into a seamless cylinder in such a way that the two points coincide. The tube can be specified by the pair of integers (L_1, L_2) that define the lattice translation vector between the two points (coordinate axes $(\bar{\mathbf{a}}_1, \bar{\mathbf{a}}_2)$) as shown in

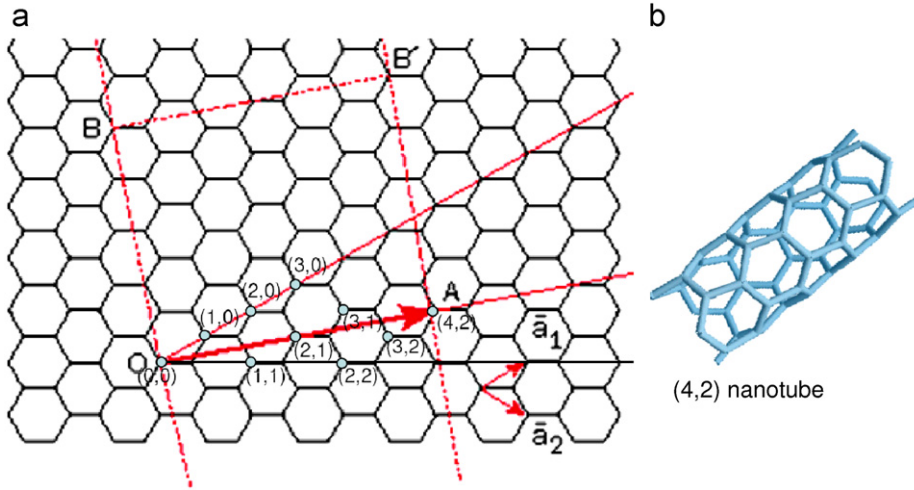


Fig. 1. The nanotube structure is obtained from a graphene sheet by rolling it up along a straight line connecting two lattice points (with translation vector (L_1, L_2)) into a seamless cylinder in such a way that the two points coincide. The figure shows how a unit cell of a (4,2) nanotube (shown in (b)) can be created by rolling the nanotube such that points O and B coincide.

Fig. 1). The nanotube can be considered as a crystal lattice with a two atom unit cell and the entire nanotube may be constructed using two screw operators (White et al., 1993). A screw operator involves a rotation of the position vector of an atom by an angle ϕ about an axis with rotation matrix S and a translation of this vector along the same axis. Any cell (\mathbf{l}) is represented by a combination $\mathbf{l} = (l_1, l_2)$. The effective operators used to obtain the cell are defined as $S(\mathbf{l}) = S_1^{l_1} S_2^{l_2}$ and $\mathbf{t}(\mathbf{l}) = l_1 \bar{\mathbf{a}}_1 + l_2 \bar{\mathbf{a}}_2$. Thus, the equilibrium position vector $\mathbf{R}(\mathbf{l}k)$ of the k th atom in the \mathbf{l} th cell is obtained from basis atoms $\mathbf{R}(\mathbf{0}k)$ as

$$\mathbf{R}(\mathbf{l}k) = S(\mathbf{l})\mathbf{R}(\mathbf{0}k) + \mathbf{t}(\mathbf{l}) \tag{5}$$

Each atom is thus uniquely represented by the pair, $\mathbf{l}k$.

A lattice-dynamical model for a SWNT can be developed using the above representation in a similar way to a 3D crystal lattice. This model was originally developed in Popov and Van Doren (2000). The equation of motion for small displacements $\mathbf{u}(\mathbf{l}k)$ of the atoms from their equilibrium positions are given by

$$m\ddot{\mathbf{u}}_i(\mathbf{l}k) = -\sum_{\mathbf{l}'k'} \Phi_{ij}(\mathbf{l}k, \mathbf{l}'k') u_j(\mathbf{l}'k') \tag{6}$$

where m is the atomic mass of carbon atom and Φ_{ij} is the force constant matrix (i, j are indices referring to x, y, z directions). The helical symmetry of the tubes necessitates wavelike solutions for the atomic displacement vectors $\mathbf{u}(\mathbf{l}k)$ (in a form similar to Eq. (5)) as follows:

$$\mathbf{u}_i(\mathbf{l}k) = \frac{1}{\sqrt{m_k}} \sum_j S_{ij}(\mathbf{l}) e_j(k|\mathbf{q}) \exp\{i[\mathbf{q} \cdot \mathbf{l} - \omega(\mathbf{q})t]\} \tag{7}$$

with wave vector $\mathbf{q} = (q_1, q_2)$, wave amplitude $\mathbf{e}(k|\mathbf{q})$ and angular frequency $\omega(\mathbf{q})$. For carbon nanotubes, in addition to the above equation, rotational boundary condition and translational periodicity constraints of the nanotube are additionally enforced (Popov and Van Doren, 2000) as $q_1 L_1 + q_2 L_2 = 2\pi l$ and $q_1 N_1 + q_2 N_2 = q$. Here, l is an integer number ($l = 0, \dots, N_c - 1$, where N_c is the number of atomic pairs in the translational unit cell of the tube), q is a new, 1D wave number, and the integers N_1 and N_2 define the primitive translation vector of the tube. The wave-vector components q_1 and q_2 can be expressed through the parameters q and l and after substituting Eq. (7) in Eq. (6), the equations of motion are obtained in the form:

$$\omega^2(q) e_i(k|ql) = \sum_{k'j} D_{ij}(kk'|ql) e_j(k'|ql) \tag{8}$$

where D_{ij} is the dynamical matrix. The equations of motion described above yield the eigenvalues $\omega(ql)$ where l labels the modes with a given wave number q ($=ka$, where a is the lattice parameter and $k = 1/\lambda$) in the 1D Brillouin zone ($-\pi < q < \pi$).

A force-constant—valence force field (VFF) model (Popov and Van Doren, 2000) of lattice dynamics which employs nearest neighbor stretch, next-to-nearest-neighbor stretch, in-plane bending, out-of-plane bending and twisting interactions was employed to compute the dispersion curves. The calculated phonon dispersion of an armchair (10,10) carbon

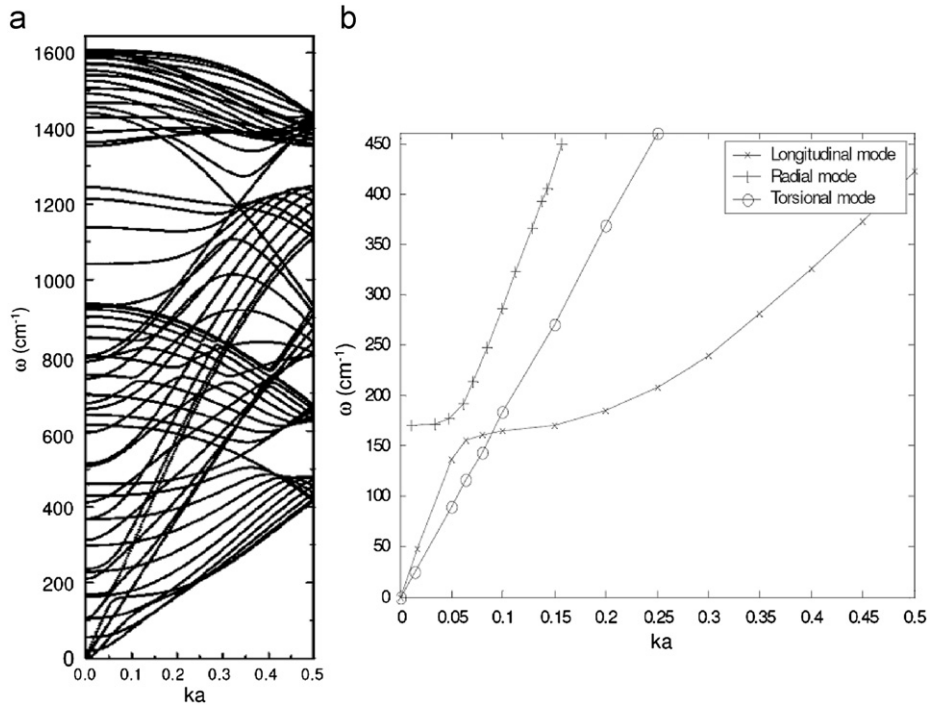


Fig. 2. (a) Atomistically computed dispersion curves for (10,10) single walled carbon nanotube. (b) The axisymmetric modes corresponding to the torsional, transverse and longitudinal vibrations of the SWCNT.

Table 1

List of constants for the (10,10) single walled nanotube.

Material constant	Value
Young's modulus E (GPa)	830
Density, ρ (kg/m ³)	2270
Poisson's ratio, ν	0.347
Bending rigidity, D (eV)	1.78
Thickness, h (nm)	0.34
Radius, r (nm)	0.678
C–C distance, a_c (nm)	0.142

nanotube in Fig. 2 shows the presence of axisymmetric longitudinal, torsional, and transverse modes at the lowest energies ($\omega < 50 \text{ cm}^{-1}$). As shown separately in Fig. 2(b), the longitudinal and torsional modes increase linearly with the wave number at large wavelengths and the transverse mode increases as the square of the wave number at large wavelengths. In this work, these axisymmetric modes will be used to identify the non-local kernel of a carbon nanotube. Further, the list of material constants used for subsequent continuum scale analysis of the nanotube (mechanical properties from the force field model, nanotube thickness and bending rigidity taken from literature Hu et al., 2008) are listed in Table 1.

3. Comparison with 1D non-local theories

The classical approach (suggested by Eringen, 1983) for reconstructing the non-local kernel is to match the dispersion curves of plane waves predicted by the non-local theory with atomistically calculated dispersion curves. Dispersion curves of a 1D axial rod model are calculated by using displacement $u(x,t)$ of the plane wave form $u(x,t) = Ue^{i(kx - \omega(k)t)}$, where k is the wave vector, and $\omega(k)$ denotes the frequency of the plane wave in the 1D governing equation $\partial s / \partial x = \rho(\partial^2 u / \partial t^2)$. For an isotropic linear elastic solid with Young's modulus (E), Poisson's ratio (ν) and density (ρ), this leads to the well-known formula (Eringen, 1983):

$$\frac{\omega}{k} = \sqrt{\frac{E}{\rho}} \sqrt{\alpha(k)} \quad (9)$$

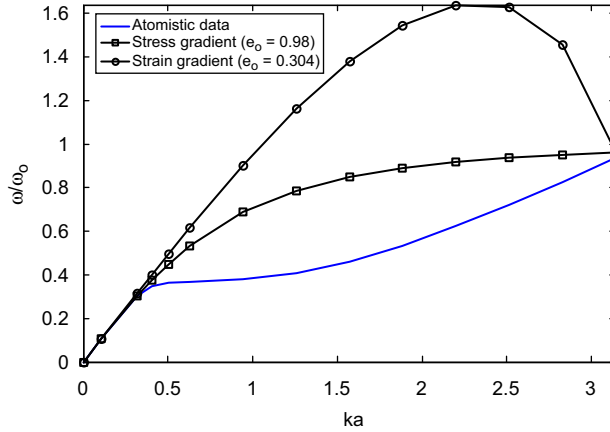


Fig. 3. Phonon dispersion curves of gradient theories are compared with the atomistically computed longitudinal mode of (10,10) nanotube.

where $\alpha(k)$ represents the Fourier transform of α .¹ Gradient theory can be derived by assuming that the kernel is of a special form that satisfies the differential equation:

$$(1 - c^2 \nabla^2) \alpha = \delta(|x|) \tag{10}$$

Substitution of the above relation in Eq. (2) results in the following constitutive equation:

$$\sigma = (1 - c^2 \nabla^2) s \tag{11}$$

As shown in Eringen, the Fourier transform of the kernel can be approximated (for $k^2 a^2 \ll 1$) as

$$\alpha(k) = \frac{2}{k^2 a^2} (1 - \cos(ka)) \cong (1 + e_0^2 a^2 k^2)^{-1} \tag{12}$$

It can be verified that this approximation indeed satisfies the above-mentioned differential equation (Eq. (10)). Eringen demonstrated that such a kernel will be able to approximate the dispersion curve of a Born Karman model ($\omega a / c_0 = 2 \sin(ka/2)$) of lattice dynamics (harmonic spring model with nearest neighbor interactions) if $e_0 = 0.39$. In Eringen’s work, fitting is performed such that the frequency predicted by the non-local elasticity model at the end of the Brillouin zone (at $ka = \pi$) is the same as the atomistic model. Alternate approaches suggested for computing the non-local parameter (e_0) in gradient theory include matching atomistic computations with theoretical predictions of continuum quantities such as elastic modulus (Wang et al., 2008) and buckling strain (Zhang et al., 2005). Zhang et al. (2005) estimated $e_0 = 0.82$ by matching the theoretical buckling strain obtained by the nonlocal thin shell model to those from molecular mechanics simulations given by Sears and Batra (2004). Following the approach of Eringen, as shown in Fig. 3, we find that $e_0 = 0.98$ best matches the longitudinal mode dispersion observed from the atomistic data. However, the group and phase velocities at smaller wavelengths ($ka > 0.5$, see Fig. 3) do not match well with atomistic predictions. In addition, we fitted the kernel ($\alpha(k)$) from atomistic data using Eq. (9). The Fourier transformed kernel from the stress gradient model ($e_0 = 0.98$) is compared directly with atomistic data in Fig. 3 and shows significant differences. The physical interpretation of these results in light of the size dependence of elastic properties of the nanotube is provided in Section 5. Next, we study the torsional and radial dispersion modes of the nanotube using shell theory in order to obtain an improved description of the kernel.

We note that another theory, namely, the strain gradient approach, has been previously used for computing the response of nanotubes. In strain gradient theory, the 1D constitutive relationship can be expressed in the form:

$$s = E \left(\varepsilon + (e_0 a)^2 \frac{\partial^2 \varepsilon}{\partial x^2} \right) \tag{13}$$

Comparison of the dispersion curve predicted by this model ($\omega/k = (\sqrt{E/\rho}) \sqrt{1 - (e_0 a)^2 k^2}$) with the atomistic dispersion curves leads to $e_0 = 0.304$. This favorably compares with the prediction of Wang and Hu (2005) who proposed $e_0 = 0.288$ within the strain gradient approach by comparing with molecular dynamics simulations. However, the theory is a second order truncation of the series represented by the gradient model (Kumar et al., 2008) and as seen in Fig. 4 does not provide a good fit to the atomistic data, over the entire range of wave numbers.

¹ $\alpha(k)$ is defined as $\int_{-\infty}^{\infty} \alpha(|x|) e^{-ikx} dx$.

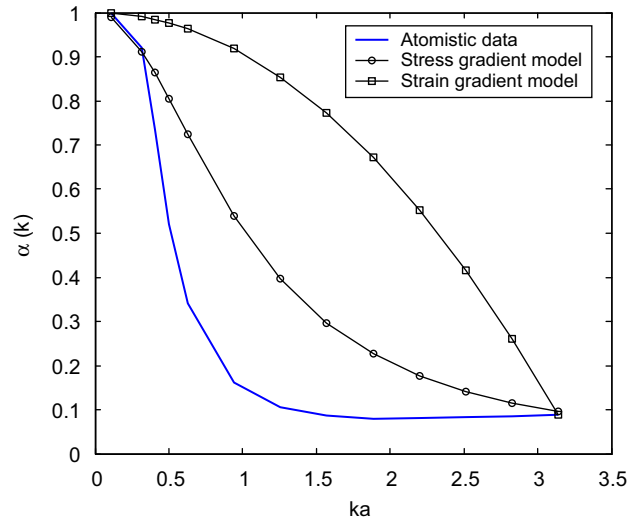


Fig. 4. The Fourier transform of the kernel computed using atomistic data and Eq. (9) is plotted against Fourier transformed kernel of (i) Stress gradient model and (ii) Strain gradient model.

4. Computation of non-local kernel using Flugge shell theory

When the radial and/or circumferential displacements dominate the wave motion, CNTs should be modeled as elastic shells rather than 1D continua in the continuum modeling approach. To establish CNT wave propagation analysis with the nonlocal elastic shell theory, a polar coordinate system is taken with x and θ denoting the longitudinal and angular circumferential coordinates. In the nonlocal elastic shell theory, the local stress and moment resultants are defined by referencing the kinematic relations in Flugge’s shell theory (Flugge, 1960) for axi-symmetric deformation ($(\partial/\partial\theta)(\cdot) = 0$)

$$N_x^l = \frac{Eh}{r(1-\nu^2)} \left(-\nu w + r \frac{du}{dx} \right) + \frac{D}{r} \frac{d^2w}{dx^2} \tag{14}$$

$$N_\theta^l = \frac{Eh}{r(1-\nu^2)} \left(-w + r\nu \frac{du}{dx} \right) - \frac{D}{r^3} w \tag{15}$$

$$N_{x\theta}^l = \frac{Eh}{2r(1+\nu)} r \frac{dv}{dx} + \frac{D}{r^2} \frac{1-\nu}{2} \frac{dv}{dx} \tag{16}$$

$$M_x^l = -\frac{D}{r^2} \left(r^2 \frac{d^2w}{dx^2} + r \frac{du}{dx} \right) \tag{17}$$

$$M_{x\theta}^l = -\frac{D}{r} (1-\nu) \frac{dv}{dx} \tag{18}$$

where $D = Eh^3/12(1-\nu^2)$ is bending rigidity in isotropic shell theory, r and h are the thickness and radius of the nanotube shell, respectively. u , v and w are displacement variables in the axial, circumferential and radial directions of the nanotube, respectively. Here, we have assumed that a isotropic description of a nanotube shell suffices at large wave numbers. The local values of the forces and moments can be used within the non-local theory to compute the kernel-averaged forces and moments. Consistent with the assumption of axisymmetric deformation, an axisymmetric kernel is utilized to describe these non-local counterparts:

$$\Gamma(\mathbf{x}) = \int_V \alpha(|\mathbf{x}-\mathbf{x}'|) \Gamma^l(\mathbf{x}') d\mathbf{x}' \tag{19}$$

The governing equations of motion in Flugge’s shell theory are (Flugge, 1960):

$$r \frac{\partial N_x}{\partial x} - \rho h r \frac{\partial^2 u}{\partial t^2} = 0 \tag{20}$$

$$r^2 \frac{\partial N_{x\theta}}{\partial x} - r \frac{\partial M_{x\theta}}{\partial x} - \rho h r^2 \frac{\partial^2 v}{\partial t^2} = 0 \tag{21}$$

$$r^2 \frac{\partial^2 M_x}{\partial x^2} + r N_\theta - \rho h r^2 \frac{\partial^2 w}{\partial t^2} = 0 \tag{22}$$

Eq. (21) represents the purely torsional motion of the shell. The plane waves representing displacements in the radial, transverse and circumferential directions are assumed to be independent of θ due to axisymmetry. Substituting the expression $v(x,t) = Ve^{i(kx-\omega t)}$ in Eq. (21), leads to the dispersion relation for torsional motion:

$$\frac{\omega}{k} = \sqrt{\frac{E}{2\rho(1+\nu)} + \frac{3D(1-\nu)}{2\rho hr^2}} \sqrt{\alpha(k)} \tag{23}$$

This dispersion relation (in terms of phase velocity) for the armchair (10,10) single walled nanotube is shown in Fig. 5. The atomistic data is compared with published molecular dynamics data (Hu et al., 2008) as well as those predicted using the local (classical) shell model ($e_0 = 0$) and the nonlocal shell models ($e_0 = 0.1, 0.2$). Similarly, substituting the expression $u(x,t) = Ue^{i(kx-\omega t)}$ and $w(x,t) = We^{i(kx-\omega t)}$ in Eqs. (20) and (22) leads to the dispersion relation for longitudinal and radial waves (where $|\cdot|$ is the matrix determinant):

$$\begin{vmatrix} \frac{\nu Eh}{r(1-\nu^2)} - \frac{Dk^2}{r} & \frac{i k E h}{1-\nu^2} - \frac{i \rho h \omega^2}{k \alpha(k)} \\ r^2 k^2 D + \frac{E h}{k^2(1-\nu^2)} + \frac{D}{r^2 k^2} - \frac{\rho h r^2 \omega^2}{k^2 \alpha(k)} & -i k r D - \frac{i E h r \nu}{k(1-\nu^2)} \end{vmatrix} = 0 \tag{24}$$

A comprehensive comparison of atomistically predicted dispersion relations for torsional, longitudinal and radial waves with those predicted by stress gradient and local elasticity ($e_0 = 0$) theories are shown in Fig. 6. Note that the torsional results in Fig. 5 (given in terms of phase velocity) are represented in terms of angular frequency in Fig. 6, for purposes of comparison. From Fig. 6(c), it is clear that the dispersion predicted by the local shell theory deviates significantly from the atomistic data at small wavelengths (for $ka > 1$). Although a calibrated stress gradient theory gives a reasonable match with atomistic data, the phase velocities (shown in Fig. 5) in the torsional mode show significant deviations at such small wavelengths. In an attempt to reconstruct the true (axisymmetric) kernel that results in the atomistically calculated dispersion curve, the Fourier transform ($\alpha(k)$) was reconstructed directly from atomistic data (based on Eqs. (23) and (24)). The results are plotted against the kernel of the stress gradient model, obtained from Eq. (12), in Fig. 7. It is seen that the gradient model involves a monotonously decreasing kernel, whereas the atomistic data predicts non-monotonous kernels that show Gaussian character. In addition, it is seen that the best-fit parameter (e_0) in gradient theory is different in the case of torsional ($e_0 = 0.16$) and longitudinal modes ($e_0 = 0.4$) indicating the anisotropic nature of the nanotube kernel. Similar values were predicted in Hu et al. (2008) by comparing molecular dynamics simulation data with shell theory. Although a real space kernel ($\alpha(x)$) corresponding to the computed Fourier transform ($\alpha(k)$) can be constructed at this point, a further study of the ability of gradient kernels to capture the effect of nanotube size on elastic properties was carried out to physically interpret these results.

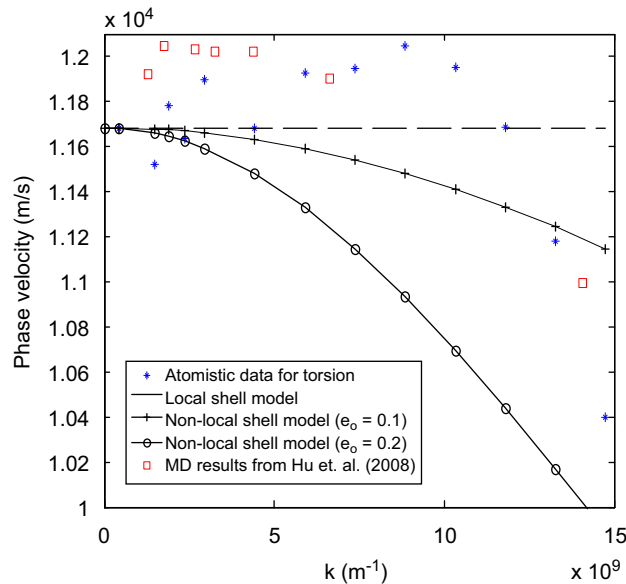


Fig. 5. Dispersion relation of torsional wave in the armchair (10,10) single walled nanotube. The atomistic data from this work is compared with published molecular dynamics data (Hu et al., 2008). The curve predicted by the local shell model ($e_0 = 0$) and the nonlocal shell models ($e_0 = 0.1$ and 0.2) are also indicated.

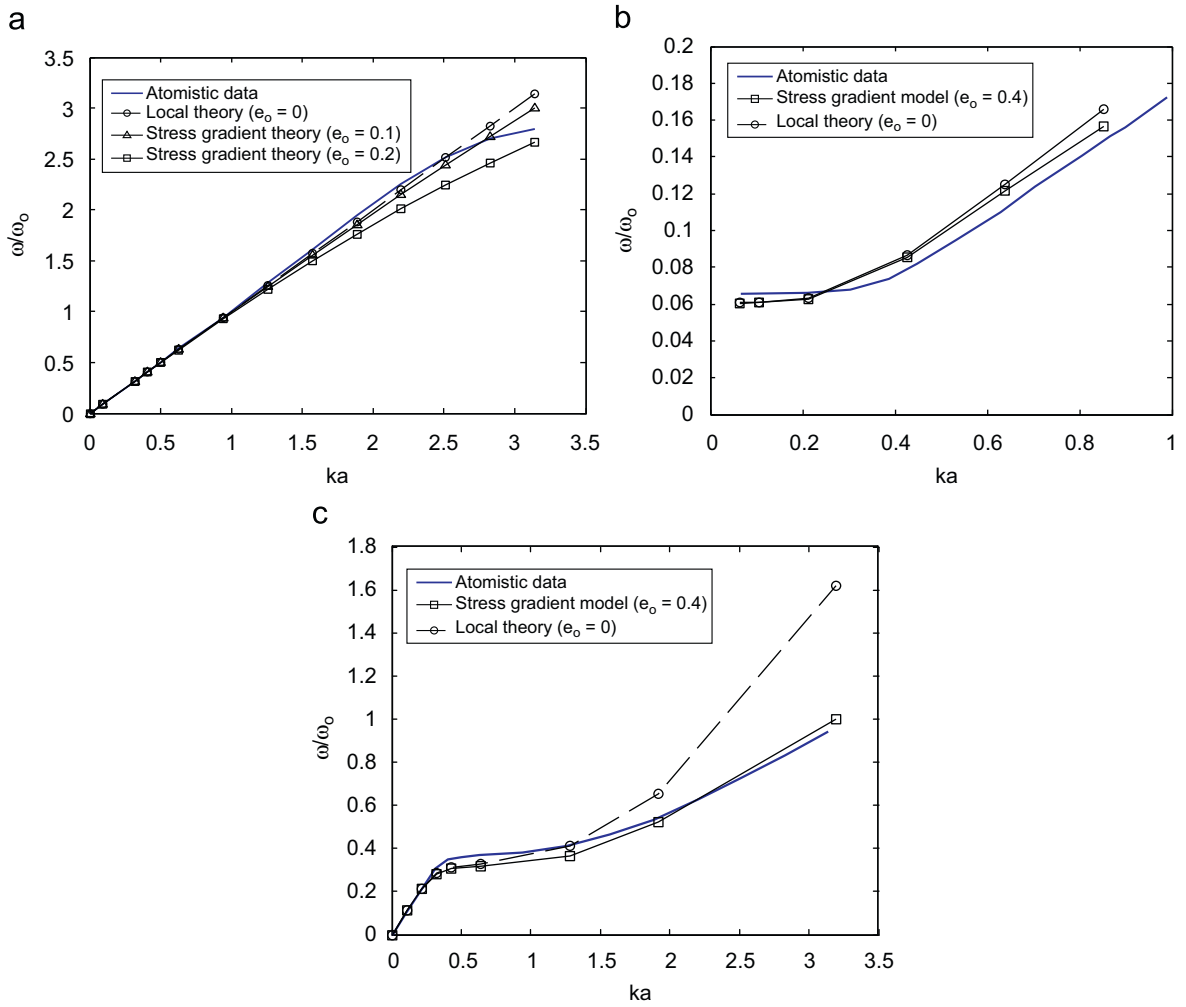


Fig. 6. Dispersion relation of (a) torsional wave (b) radial (transverse) wave and (c) longitudinal wave in the armchair (10,10) single walled nanotube. The curve predicted by the local (classical) shell model ($e_0 = 0$) and nonlocal shell models are indicated.

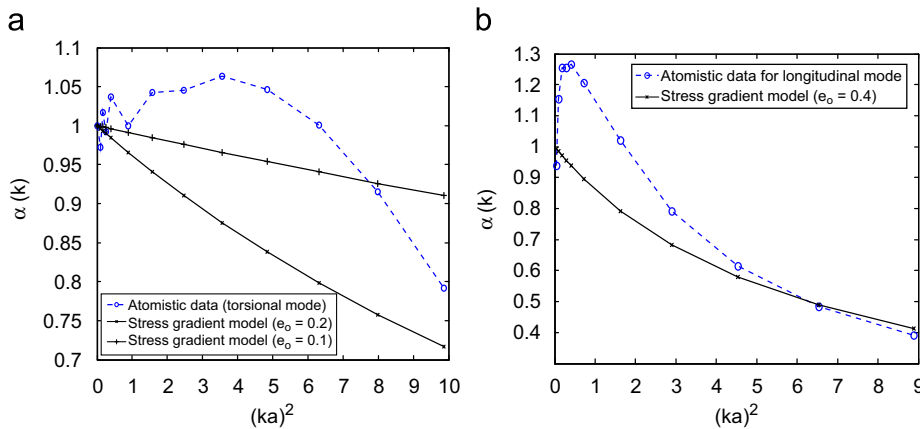


Fig. 7. The Fourier transform of the kernel computed using atomistic data is plotted against the kernel of the stress gradient model for (a) Torsional mode and (b) Longitudinal mode.

5. Physical interpretation of kernels

A significant advantage of gradient approaches over local theories is the ability to capture size effects. To further test the physical interpretation of the kernel parameters, we have performed detailed comparisons of theory with atomistically measured variation of elastic moduli and shear moduli with length of the nanotube. Such an experiment was performed in Wang et al. (2008), however, the experiment was stress-controlled and the approach required non-trivial displacement solution of the non-local model for comparison. Alternatively, displacement controlled tests can be performed and the displacements can be directly substituted into the gradient model to compare energy variations with the atomistic data. Following this latter approach, the atomistic measurement involved applied displacement on nanotubes of various lengths from $L = 10$ to 70 \AA . Two types of tests, tension and torsion, were conducted. In the first test, uniform tensile strain of 0.0001 was applied to the nanotube by perturbing each atom by a small displacement along the x -direction as shown in Fig. 8(a). In another experiment, the nanotube was subjected to a torsion test with a constant rate of twist of 0.0001 rad/m as shown in Fig. 8(b). The changes in energies (ΔE) of the deformed case with respect to the undeformed case was noted. The elastic modulus (E) and shear modulus (G) of nanotubes of different lengths are computed assuming (1) isotropic properties and (2) constant cross sectional properties (area (A), polar moment of inertia (J)) for nanotubes of various lengths. In classical local theory, the change in energy of a tube subjected to tension and torsion, respectively, are given as $\Delta E = \frac{1}{2}EAL\epsilon^2$ and $\Delta E = \frac{1}{2}GJL\theta^2$, respectively. Given that parameters A , J , ϵ and θ do not change with the length of the nanotube, the elastic moduli and shear moduli can be computed as a function of length by measuring the energy change (ΔE) using atomistic data and plotting the normalized variation of the factor $\Delta E/L$. The same energy change can be predicted from 1D rod and axisymmetric shell theories as follows:

Non-local 1D rod theory—tension test: The strain energy change during a tension test is given by

$$\Delta E = \frac{A}{2} \int_0^L \left\{ \int_V (\alpha(x-x^*)E \frac{\partial u}{\partial x^*} dx^*) \right\} \frac{\partial u}{\partial x} dx \quad (25)$$

The displacements are already known from the atomistic test. The conditions used in the simulation are (i) $\partial u/\partial x = 0.0001$ for $x > 0$ and $x < L$ and (ii) $\partial u/\partial x = 0$ elsewhere. These values are substituted in the above expression and the energy changes are plotted along with atomistic simulation results in Fig. 9. Various curves can be obtained for the size effect by varying the value of a single parameter $e_0 a$ in the stress gradient theory. The simulations from stress gradient theory compare well with atomistic results at $e_0 a = 2.03 \text{ \AA}$. Using the lattice parameter of the translational unit cell (2.4566 \AA) for (10,10) nanotube, the parameter e_0 can be inferred to be 0.8263, which agrees remarkably well with the prediction of Zhang et al. (2005) ($e_0 = 0.82$ using elastic buckling theory). The reason for the good match is that, in both cases, the gradient theory parameter was computed in the context of elasticity theory (albeit using buckling strain in Zhang et al., 2005 and size effect of elastic moduli in this new study) without resorting to lattice dynamics. However, from these results (based on $e_0 = 0.98$ obtained from the phonon dispersion curve), it is evident that stress gradient theory, with a single parameter, cannot fully describe both the dynamics of the single walled nanotube and the size effect of moduli.

Non-local shell theory—torsion test: The energy change in the torsion test is predicted using non-local shell theory. For the torsion test, the displacement constraints are (i) $u = w = 0$, (ii) $\partial v/\partial x = \text{constant}$ for $x > 0$ and $x < L$ and (iii) $\partial v/\partial x = 0$ elsewhere. The energy change is given by the following expression:

$$\Delta E = \frac{A \left(1 + \frac{h^2}{4a^2}\right)}{2} \int_0^L \left\{ \int_V (\alpha(x-x^*) \frac{E}{2(1+\nu)} \frac{\partial v}{\partial x^*} dx^*) \right\} \frac{\partial v}{\partial x} dx \quad (26)$$

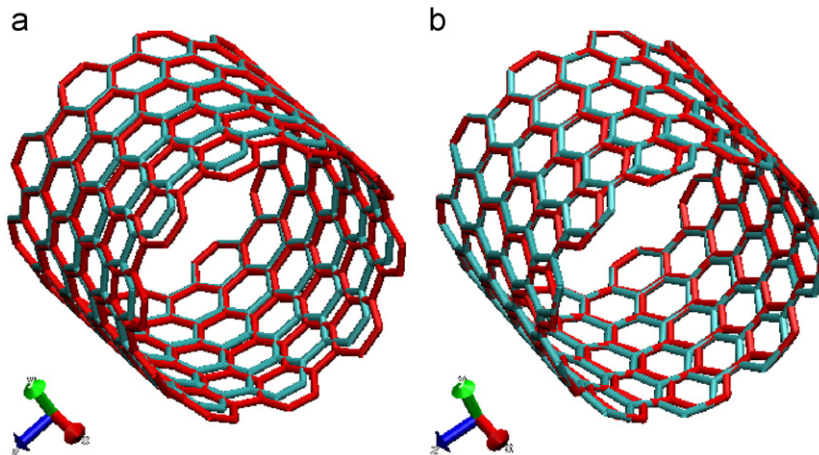


Fig. 8. Displacement-controlled (a) tension test and (b) torsional test configurations on a (10,10) single walled carbon nanotube. Displacements have been exaggerated for visualization.

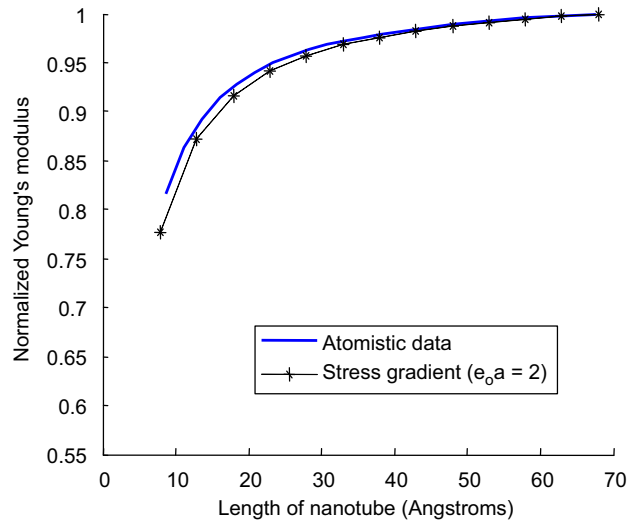


Fig. 9. Length dependence of axial modulus obtained from the atomistic simulation is compared with the results of stress gradient model at $e_o a = 2 \text{ \AA}$.

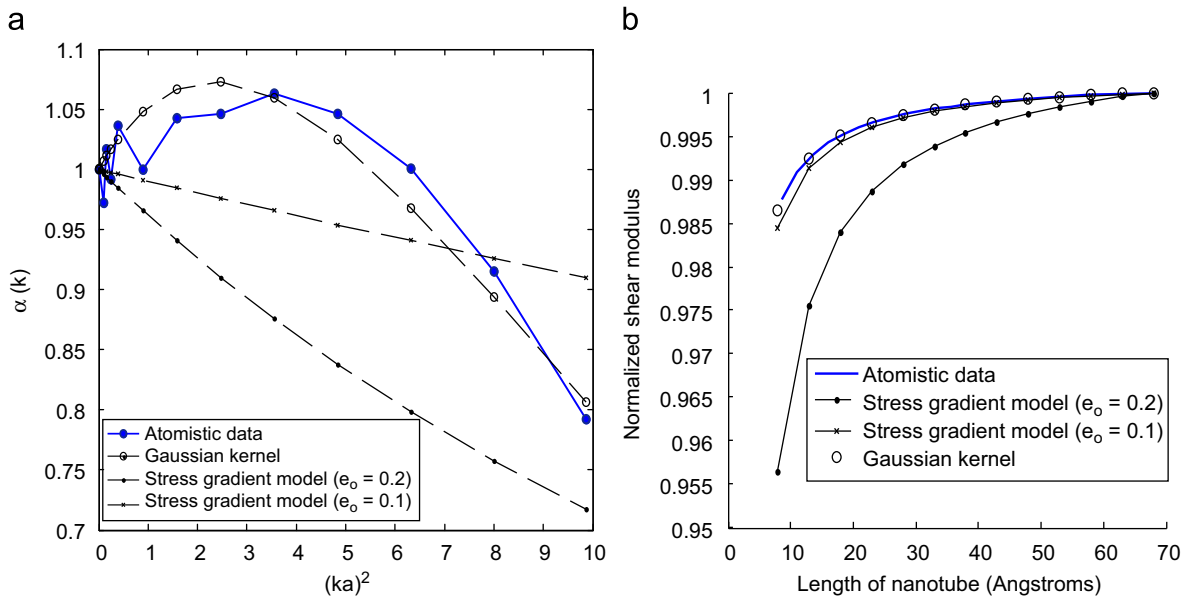


Fig. 10. (a) The Fourier transform of the kernel computed using atomistic data for torsional mode (computed from Eqs. (23)) is plotted against the kernels of the stress gradient model (for $e_o = 0.1, 0.2$) and the new Gaussian kernel. (b) Length dependence of shear modulus obtained from the atomistic simulation is compared with the results of stress gradient models and the new Gaussian kernel.

Consolidating our results from the phonon dispersion study and size effect study, we have shown both the Fourier transformed kernel and the size effect in shear modulus predicted by the non-local shell theory and atomistic data in Fig. 10. The simulations from stress gradient theory compare well with atomistic data of size effect at $e_o = 0.1$. However, gradient theory with $e_o = 0.1$ does not predict the atomistic dispersion curve adequately. Again, from the results in Fig. 10, it is evident that stress gradient theory, with a single parameter, cannot fully describe both the dynamics of the single walled nanotube and the size effect, simultaneously. To get a sense of the real non-local kernel of the carbon nanotube, we attempted to fit the data to a new kernel. Several popular forms of the 1D kernel (presented in Eringen, 1983) can be chosen for the fitting process. For demonstration, we proceeded with a simple form of the kernel parameterized as a sum of Gaussians.

In Fig. 10(a), we have plotted the Fourier transformed parameters of the best fit Gaussian-type kernel which provides a reasonable description of the atomistic data. The Fourier transform of the kernel obtained from atomistic data is given by the following function:

$$\alpha(k) = -0.0917 + 1.6931 \exp(-(ka)^2/16.5454) - 0.6014 \exp(-(ka)^2/3.4479) \tag{27}$$

The improved prediction of size effect in shear modulus by this Gaussian kernel is shown in Fig. 10(b). The real space reconstruction of the kernel (in real space, as used in the size effect analysis) is as follows (where $y = |\mathbf{x}' - \mathbf{x}|$ is in Angstrom units):

$$\alpha(y) = -0.0917\delta(y) + 0.9121\exp(-(y/1.0473)^2) - 0.1479\exp(-(y/2.2942)^2) \quad (28)$$

In Fig. 11, the stress gradient model kernel and the reconstructed Gaussian kernel are directly compared. In contrast to the stress gradient theory, it is seen that best-fit kernel weights become negative at larger distances. These effects have been previously seen in the kernels reconstructed by Picu (2002) for metallic systems. Physically, the non-local kernel captures the effect that stresses applied on neighboring atoms have on the central atom. A positive strain on the nearest neighbor atom will increase the stress on the central atom. However, if an atom located beyond the inflection point (of the interatomic potential) is given a positive strain, the stress on the central atom will decrease. To capture this effect, the kernel has to become negative at a certain distance from the central atom. This effect is not captured by the stress gradient theory, however improved kernels as presented here (eg. Eq. (28)) captures this effect. The location of the inflection point for the nanotube is confirmed next through an atomistic study of layer-by-layer interaction of atoms in a carbon nanotube.

In order to compute the effective 1D interaction potential along the nanotube, we model the nanotube as a chain of particles joined together with springs. In this 1D model, each particle represents a layer of atoms in the nanotube (numbered 0,1,2,3 as shown in Fig. 12(a)) and are arranged with a lattice distance of 1.23 Å. Let k_1 be the linear spring constant for nearest neighbor interaction under infinitesimally small displacements. Similarly, k_2, k_3, \dots are the constants for second neighbor springs, third neighbor springs etc as shown in Fig. 12(a)). The effective interaction energies were computed from a series of tests on a 70 Å long nanotube model. The procedure to find the energy associated with spring k_2 is as follows:

1. Compute the energy of the unperturbed system (E_1)
2. Perturb layer 2 by $\delta = 0.1$ Å and compute the energy (E_2)
3. Remove layer 0 and compute the energy (E_3)
4. Remove layer 0, perturb layer 2 by $\delta = 0.1$ Å and compute the energy (E_4)

Energy E_1 is measured for a relaxed (ground state) nanotube system. Rest of the tests were carried out without relaxing the perturbed system. The energy for the interaction between layers 0 and 2 of the nanotube is then given by the

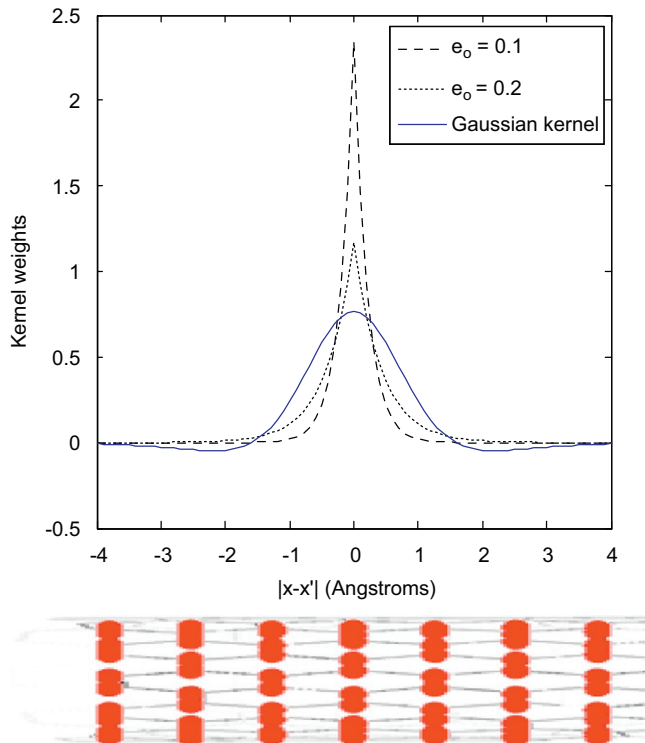


Fig. 11. The best fit Gaussian-type kernel obtained from atomistic data of the torsional mode is compared with stress gradient theory kernels (in real space). Reconstructed kernel weights are plotted as a function of distance from a central location at $x = x'$. Kernel weights of the best fit kernel become negative at larger distances (also Picu, 2002). The (10,10) nanotube is inset to give an idea of how the kernel weights vary with atom locations in a nanotube.

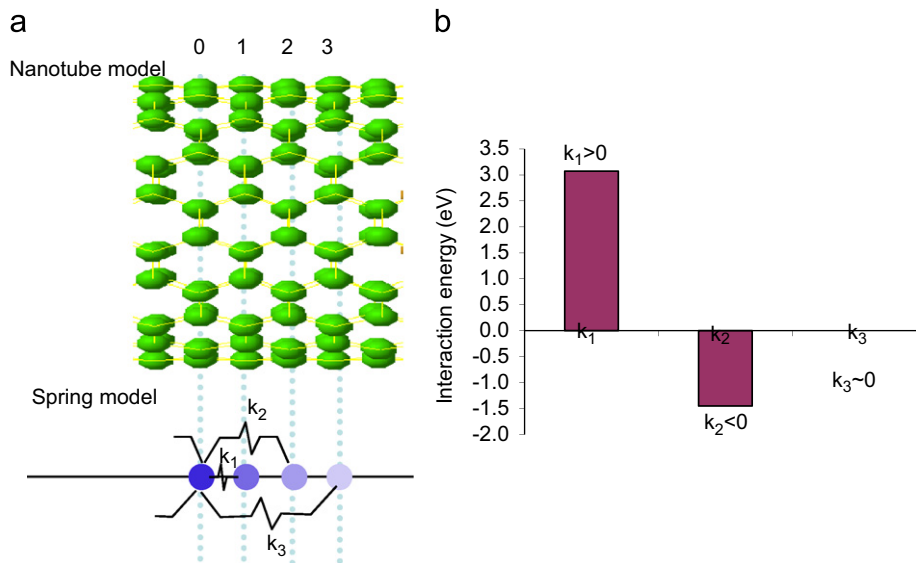


Fig. 12. (a) A spring model has been constructed to simulate the nanotube. In this 1D model, atoms within each layer in the nanotube (numbered 0 through 3) are coarse grained as a single atom. The interaction energies corresponding to springs (k_1, k_2, k_3) are computed from atomistic simulations. (b) The computed energies are indicated. It is seen that the energy is positive for 0–1 interaction and is negative for 0–2 type interaction.

expression $\Delta E_{0-2} = E_2 + E_3 - E_4 - E_1$. Similar procedures were carried out to compute the energies associated with springs k_1 and k_3 . The computed interaction energies are indicated in Fig. 12(b). It is seen that the energy is positive for 0–1 interaction and is negative for the 0–2 type interaction. This confirms our observation in Fig. 11 where the kernel fitted to atomistic data leads to negative weights at the second layer of atoms and gives an interpretation of the nature of the non-local kernel.

6. Conclusions

The longitudinal, transverse and torsional axisymmetric mode wave dispersions in single walled carbon nanotube (SWCNT) were studied in the context of nonlocal elasticity theory. The dispersion data for an armchair (10,10) SWCNT was obtained from lattice dynamics of SWNTs while accounting for the helical symmetry of the tubes. The data was used to compare with predictions of popular (stress- and strain-) gradient theories and to gain better insight into the physical nature of the non-local elasticity kernel. In this regard, the following observations were drawn:

1. The approach of Eringen was used to predict the material parameter (e_0) in gradient theory. This is done by matching the frequency predicted by the non-local elasticity model at the end of the Brillouin zone to the atomistic model for 1D continuum and axisymmetric cylindrical shell continuum model of a nanotube. The predicted data agree reasonably well with various elasticity based results published in literature (Wang and Hu, 2005; Hu et al., 2008). However, it is seen that stress and strain gradient model incur significant errors in both the phase and group velocity when compared to the atomistic model.
2. To further test the gradient theories, we provided a detailed atomistic study of size effect in nanotubes. The size effect predicted by 1D stress gradient theory agrees well with the atomistic data for a value of $e_0 a = 2.03 \text{ \AA}$ and reconfirm the prediction of Zhang et al. (2005). However, it is evident that stress gradient theory kernels, with a single parameter ($e_0 a$), cannot fully describe both the complex lattice dynamics of the single walled nanotube and the size effect in shear moduli.
3. In order to gain a better physical insight on the nature of the non-local kernel, we fitted a new kernel from the atomistic data. We see that unlike the kernel from gradient theory, the kernel fitted from atomistic data becomes negative at larger distances from the reference point.
4. We postulated and confirmed that the fitted kernel changes sign close to the inflection point of the interatomic potential through an atomistic study of layer-by-layer interaction of atoms in a carbon nanotube.

In this preliminary study, 1D kernels (in axial or axisymmetric modes) within isotropic constitutive description have been considered. In general, a variety of deformation modes needs to be tested and elastic anisotropy of the nanotube have to be considered to develop a fully 3D form of the non-local kernel. In addition, as deformation proceeds, the form of the non-local kernel (eg. the inflection point) is expected to change as atoms redistribute and relax. The techniques mentioned

in this paper will be useful to parameterize the kernel in terms of deformation for use in continuum simulations of failure of nanotubes and nanotube impregnated composites. Work in these areas are underway.

References

- Aifantis, E.C., 1999. Strain gradient interpretation of size effects. *Int. J. Fracture* 95 (1–4), 299–314.
- Eringen, A.C., 1983. On differential equations of nonlocal elasticity and solutions of screw dislocation and surface waves. *J. Appl. Phys.* 54, 4703–4710.
- Flügge, W., 1960. *Stresses in Shells*. Springer, Berlin/Heidelberg.
- Hu, Y.-G., Liew, K.M., Wang, Q., He, X.Q., Yakobson, B.I., 2008. Nonlocal shell model for elastic wave propagation in single- and double-walled carbon nanotubes. *J. Mech. Phys. Solids* 56 (12), 3475–3485.
- Kumar, D., Heinrich, C., Waas, A.M., 2008. Buckling analysis of carbon nanotubes modeled using nonlocal continuum theories. *J. Appl. Phys.* 103, 073521.
- Peddieon, J., Buchanan, G.R., McNitt, R.P., 2003. Application of nonlocal continuum models to nanotechnology. *Int. J. Eng. Sci.* 41, 305–312.
- Picu, R.C., 2002. On the functional form of non-local elasticity kernels. *J. Mech. Phys. Solids* 50 (9), 1923–1939.
- Popov, V.N., Van Doren, V.E., 2000. Elastic properties of single-walled nanotubes. *Phys. Rev. B* 61 (4), 3078–3084.
- Sears, A., Batra, R.C., 2004. Macroscopic properties of carbon nanotubes from molecular-mechanics simulations. *Phys. Rev. B* 69, 235406.
- Sudak, L.J., 2003. Column buckling of multiwalled carbon nanotubes using nonlocal continuum mechanics. *J. Appl. Phys.* 94 (11), 7281.
- Sun, C.T., Zhang, H., 2003. Size-dependent elastic moduli of platelike nanomaterials. *J. Appl. Phys.* 93, 1212–1218.
- Wang, L.F., Hu, H.Y., 2005. Flexural wave propagation in single-walled carbon nanotubes. *Phys. Rev. B* 71, 195412.
- Wang, Q., Varadan, V.K., 2007. Application of nonlocal elastic shell theory in wave propagation analysis of carbon nanotubes. *Smart Mater. Struct.* 16, 178–190.
- Wang, C.Y., Ru, C.Q., Mioduchowski, A., 2005. Axisymmetric and beamlike vibrations of multiwall carbon nanotubes. *Phys. Rev. B* 72 075414(1–10).
- Wang, L., Zheng, Q., Liu, J.Z., Jiang, Q., 2005. Size dependence of the thin-shell model for carbon nanotubes. *Phys. Rev. Lett.* 95 105501(1–4).
- Wang, Q., Han, Q.K., Wen, B.C., 2008. Estimate of material property of carbon nanotubes via nonlocal elasticity. *Adv. Theor. Appl. Mech. (online)* 1 (1–4), 1–10.
- White, C.T., Robertson, D.H., Mintmire, J.W., 1993. Helical and rotational symmetries of nanoscale graphitic tubules. *Phys. Rev. B* 47, 5485.
- Zhang, Y.Q., Liu, G.R., Xie, X.Y., 2005. Free transverse vibration of double-walled carbon nanotubes using a theory of nonlocal elasticity. *Phys. Rev. B* 71, 195404.